
Laminar natural convection of power-law fluid in a differentially heated inclined square cavity

Horimek Abderrahmane^{1,*}, Nouredine Brahim¹, Benkhchiba Abdelfatah¹, Ait-Messaoudene Noureddine²

1. Laboratoire de Développement en Mécanique et Matériaux (LDM2)
Djelfa University, Algeria

2. Department of Mechanical Engineering, Faculty of Engineering
University of Hail, KSA

Horimek_aer@yahoo.fr

ABSTRACT. *The objective of this work is the study the problem of laminar natural convection, for a power-law fluid, in a differentially heated square cavity, to which a clockwise or counterclockwise inclinations are attributed compared to the classical case ($\phi=0^\circ$). A finite volume code was used to make the simulations. The study was divided into several parts in order to distinguish the effects of the different widely-varied' parameters included (Rayleigh number Ran [$10+3 \rightarrow 10+6$], rheological index n [$0.6 \rightarrow 1.8$], inclination angle ϕ [$-90^\circ \rightarrow 90^\circ$] and Prandtl number Prn [$10 \rightarrow 10+4$]) independently and combined. The obtained results showed the increase of dynamic and thermal fields disturbances for increasing Ran and/or decreasing n especially for a counterclockwise inclination (over a range of variation), with improvement of the heat exchange coefficient, particularly at high Prn . The opposite will occur when Ran decreases and/or n increases and becomes clearer for a clockwise inclination. In addition, an optimal angle for a counterclockwise inclination is recorded (highest mean heat transfer coefficient). This angle is influenced by Ran increase and n decrease. Recommended ranges of inclination angles leading to highest heat transfer rate are finally given depending on problem parameters. The industrial exploitation of the recommended ranges, undoubtedly allows benefits of efficiency and/or economy.*

RÉESUMÉ. *Cet article a pour but d'étudier le problème de la convection naturelle laminaire, pour un fluide de loi de puissance, dans une cavité carrée chauffée de manière différentielle, à laquelle sont attribuées des inclinaisons dans le sens horaire ou antihoraire par rapport au cas classique ($\phi = 0^\circ$). Un code de volume fini a été utilisé pour effectuer les simulations. L'étude a été divisée en plusieurs parties afin de distinguer les effets des différents paramètres très variés inclus (nombre de Rayleigh Ran [$10 + 3 \rightarrow 10 + 6$], indice rhéologique n [$0,6 \rightarrow 1,8$], angle d'inclinaison ϕ [$- 90^\circ \rightarrow 90^\circ$] et le nombre de Prandtl Prn [$10 \rightarrow 10 + 4$]) indépendamment et combinés. Les résultats obtenus ont montré l'augmentation des perturbations des champs dynamiques et thermiques pour augmenter Ran et / ou diminuer n , en particulier pour une inclinaison dans le sens antihoraire (sur une plage de variation), avec*

amélioration du coefficient d'échange thermique, en particulier à forte Prn. L'inverse se produira lorsque Ran diminue et / ou n augmente et devient plus clair pour une inclinaison dans le sens des aiguilles d'une montre. De plus, un angle optimal pour une inclinaison dans le sens antihoraire est enregistré (coefficient de transfert thermique moyen le plus élevé). Cet angle est influencé par l'augmentation de Ran et la diminution de n. Les plages d'angles d'inclinaison recommandées conduisant au taux de transfert de chaleur le plus élevé sont finalement indiquées en fonction des paramètres du problème. L'exploitation industrielle des gammes recommandées permet sans aucun doute des avantages d'efficacité et / ou d'économie.

KEYWORDS: *natural convection, square cavity, inclination angle, power-law fluid, prandtl number.*

MOTS-CLÉS: *convection naturelle, cavité carrée, angle d'inclinaison, fluide loi de puissance, nombre de Prandtl.*

DOI:10.3166/ACSM.41.261-281 © 2017 Lavoisier

1. Introduction

Natural convection inside square cavity is one of the most studied problems in heat transfer literature. The first published works date back to about sixty (60) years. The extensive review made by Ostrach (1972) and Yener *et al.* (2013) neatly captures in a chained manner the available works from 1953 till 2013. This kind of problems is widely found in practice for Newtonian and Non-Newtonian fluids. Oil-drilling, pulp paper, slurry transport, food processing, polymer engineering (Khezzar *et al.*, 2012), geophysical systems, electronic cooling systems, and nuclear reactors are examples for both types of fluids (Raisi, 2016).

In the following; only relevant works of our study will be presented. For a non-Newtonian fluid, Ozoe and Churchill (1972) were the first to study natural convection of power-law fluids (Ostwald-de Waele and Ellis models), in a bidimensional square cavity heated from bellow. A stabilization algorithm was proposed to predict the critical Rayleigh number (transition limit). Finite difference technique was employed. Time and space steps were carefully discussed. Lot of relevant works have been published afterwards, dealing with other aspects to improve or amplify the known results (Ohta *et al.*, 2002; Kaddiri *et al.*, 2012). For a laminar regime, many works are published as-well. Turan *et al.* (2011b) have studied the problem in a square cavity with two vertical walls at different imposed temperatures and adiabatic horizontal ones. Wide variations ranges of the various intervening parameters (Ra , n , and Pr) are supposed. A scaling analysis, made by authors, allows reformulating Ra , Gr and Pr expressions, where n is brought out. Many interesting results were provided. They have showed that the Pr effect on heat transfer rate is negligible for $n > 1.0$ even at high Ra , while it is no longer negligible at small n ($=0.6$) for $Pr < 10^{+2}$ if Ra exceeds 10^{+4} (for further details, see Koca *et al.*, 2007). Finally, they have proposed two expressions for mean Nusselt number, the first for n ranging between 0.6 and 1.8, while the other is for $n \leq 1.0$. Using the same methodology, the authors have assumed the case of vertical walls at imposed heat flux instead of imposed temperatures (Turan *et al.*, 2012). They have showed that heat transfer rate for the new thermal condition, is lower than that for imposed

temperatures. The difference is more pronounced when n is smaller. As done before, they have proposed an expression for mean Nusselt number as function of n .

For square inclined cavity and Newtonian fluid; Huelsz and Rechtman (2013), have used the Lattice-Boltzman technique to solve the problem for air as heating fluid. Inclination angle was ranged from 0° to 180° , and from -180° to 0° . This is the reason why they have obtained symmetrical curves for mean Nusselt number and velocity v_1 (vertical velocity at $x=0.9$ and $y=0.5$), compared to the case with 0° , corresponding to hot top wall (T_H) and cold bottom wall (T_C). The remaining walls are kept adiabatic. Several results were presented. Authors have showed that mean heat transfer coefficient, takes his highest value between 55° and 84° for Ra ranging from 10^{+3} to $2 \times 10^{+6}$. Is it worth to notice that from $Ra=O(10^{+5})$ and higher, the highest values are all close to 84° , which corresponds to 6° of deviation to the left, from the situation, where the hot wall is vertical. These recorded results are verified in our present work, with extension to non-Newtonian case. For a local Nusselt, interested reader may refer to the work of Hamady *et al.* (1989), where its results for different inclination angles for $Ra=1.1 \times 10^{+5}$ are given, and the work of Rasoul and Prinos (1997), for more extended and interested results. For an inclined rectangular cavity, Vingradov *et al.* (2011), have studied this case for two aspect ratios ($AR=L/H$) equal to 1 and 4 respectively, for $Ra=10^{+5}$ and $Pr=10^{+2}$. Three values of the rheological index ($n=0.6, 1.0$ and 1.4) are considered for a counterclockwise inclination ranging from 0° to 90° (Top wall at T_C , Bottom to T_H and the two remaining, adiabatic). The study is extended later for the cases $Ra=10^{+4}$ at $Pr=10^{+3}$ and 10^{+4} (cf Khezzar *et al.*, 2012). Two other values of n are examined ($n=0.8$ and 1.2) with a new added AR ($AR=8$). Both studies, showed improvement of heat exchange with increasing Ra and/or decreasing n , in addition to the existence of an optimal angle offering the maximum heat exchange rate. Furthermore, authors have presented results showing the existence of a singularity angle for the mean Nusselt number, when AR becomes different of 1.0. The angle magnitude and the singularity sharpness depend on n and Ra . The extension of variations' ranges of the different involved parameters seems necessary to well understand the phenomena recorded. More details can be found in the author's work (Khezzar *et al.*, 2011). Turan *et al.* (2011a), have studied extensively the point, for non-inclined rectangular cavity for air and water for the same boundary conditions supposed in Turan *et al.* (2012). In a subsequent work, Turan *et al.* (2013) have supposed a power-law fluid instead of Newtonian one. Pr number was taken equal to 10^{+3} . We can summarize that; mean Nusselt number increases for imposed temperatures at vertical walls, until a maximum values and then decreases, while it increases monotonically for imposed heat flux condition. AR_{max} (AR for optimal mean Nusselt number) depends on Ra , Pr and n . For both last works AR was ranged from 0.125 to 8.0. For an inclined square cavity but with a Bingham (Bn) non-Newtonian fluid, Ygit *et al.* (2013) have showed that heat transfer rate increases until a certain angle then decreases. We note that, they have supposed an inclination angle ranging from 0° to 180° , where the initial position was with a horizontal hot bottom wall (T_H) and cooled top one (T_C) for vertical adiabatic ones. Authors have also showed that heat exchange declines with an increasing Bn , and it becomes purely conductive from a

certain value. This latter is influenced by inclination and Ra . Works dealing with nanofluid, in Newtonian or non-Newtonian behaviors are intentionally avoided.

From the above mentioned literature survey, one can see the lack of works treating inclined square (and rectangular) cavities, for power-law fluids in laminar regime. The only works we were able to find, are those of Vingradov *et al.* (2011) and Khezzar *et al.* (2012), which are limited to $n \leq 1.4$, in addition to an inclination angle ranging from 0° to 90° (corresponding to: from -90° to 0° in our study) and $Ra_{max} = 10^{+5}$. Consequently, in the current study we have supposed a square inclined cavity, filled with a power-law non-Newtonian fluid, and differentially heated with constant temperatures at two opposite walls, while the others are kept adiabatic. For better analysis of the included parameters' effects, wide ranges of variations are assumed. Rayleigh number (Ra_n) is varied from 10^{+3} to 10^{+6} ; rheological index (n), from 0.6 to 1.8; inclination angle (ϕ) from -90° to $+90^\circ$, with small step of variation and finally, Pr_n number from 10 to 10000. We note that the chosen ranges, allow us to not only well analyze the parameters' effects, but to also cover almost all possibly existing cases in practice. Ra_n range of variation, starts from a nearly pure-conductive heating mode, to that close to the turbulence transition' limit. n index variation' range covers, pseudoplastic fluids (<1.0), Newtonian fluid ($=1.0$) and dilatant fluids (>1.0). We note that few works have supposed such a wide range (Turan *et al.*, 2011b; 2012; Yigit *et al.*, 2016). We recall that pseudoplastic fluid with $n < 0.6$ is considered extremely shear-thinning (Viscosity decreases under shear application), and is similar in some ways to yields stress fluid (Yigit *et al.*, 2016). In addition, this feature generates numerical instabilities, by the presence of very low viscosity magnitudes, especially at high Ra . Therefore, the possibility of not being in laminar flow may occur. By contrast, heat transfer becomes very weak when viscous friction caused by viscosity increase grows for $n \geq 1.8$, even at high Ra_n . No interest in taking values larger than 1.8 occurs. Inclination angle range, covers all possible situations. It starts from the classical case with $\phi = 0^\circ$ where vertical walls are heated. It is done in clockwise direction until $\phi = -90^\circ$ and also in anticlockwise direction at $\phi = +90^\circ$. The small angle step taken (5°), allows us to well analyze the resulting phenomena and the mean Nusselt number calculation. Finally, the Pr_n range of variation, allows firstly to illustrate its effect, and secondly it covers a wide range of fluids in practice, hence the importance of the results provided. Moreover and as detailed above, there is an optimal inclination angle, corresponding to a maximum heat transfer rate. This was not well studied before. In this work we will try to show the dependence of this angle on the different parameters of the problem in a clear manner, for the purpose of its practical exploitation.

2. Problem description

It is a natural convective heat transfer problem inside a square inclined enclosure, filled with non-Newtonian power-law fluid. The cavity inclination angle varies from -90° to $+90^\circ$ compared to the vertical position ($\phi = 0^\circ$). Left and right sides are at fixed temperatures (with respect to the initial position), where the left one is hot (T_H) and the right one is cold (T_C). The remaining sides are insulated (Figure 1).

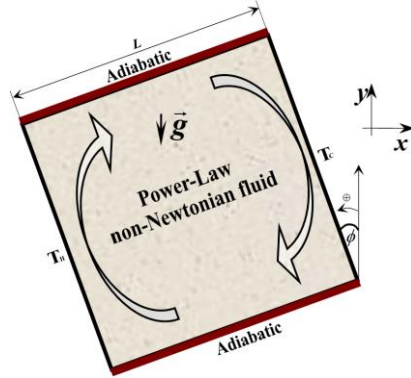


Figure 1. Problem geometry

Flow is assumed laminar, steady and two dimensional. Boussinesq approximation is adopted. Viscous dissipations are supposed negligible. Other fluid physical parameters are assumed to be constant except viscosity, supposed to be shear-dependent. Following the previous considerations, continuity, x -momentum, y -momentum and energy equation of the problem are written as follows:

$$\frac{\partial u_1}{\partial x} + \frac{\partial u_2}{\partial y} = 0 \tag{1}$$

$$u_1 \frac{\partial u_1}{\partial x} + u_2 \frac{\partial u_1}{\partial y} = -\frac{1}{\rho_{ref}} \frac{\partial p}{\partial x} + \frac{1}{\rho_{ref}} \left(\frac{\partial \tau_{xx}}{\partial x} + \frac{\partial \tau_{xy}}{\partial y} \right) \pm g\beta(T - T_{ref}) \sin \phi \tag{2}$$

$$u_1 \frac{\partial u_2}{\partial x} + u_2 \frac{\partial u_2}{\partial y} = -\frac{1}{\rho_{ref}} \frac{\partial p}{\partial y} + \frac{1}{\rho_{ref}} \left(\frac{\partial \tau_{xy}}{\partial x} + \frac{\partial \tau_{yy}}{\partial y} \right) - g\beta(T - T_{ref}) \cos \phi \tag{3}$$

$$u_1 \frac{\partial T}{\partial x} + u_2 \frac{\partial T}{\partial y} = k \left(\frac{\partial^2 T}{\partial x^2} + \frac{\partial^2 T}{\partial y^2} \right) \tag{4}$$

u_1 and u_2 are velocity components flowing x and y directions. p , T , ϕ , g and k are pressure, temperature, thermal expansion coefficient, gravity acceleration and thermal conductivity respectively. The index *ref* indicates reference values.

Since the fluid is supposed non-Newtonian, viscosity is no longer constant inside the enclosure. Different mathematical (rheological) models can be found in literature. In the present study, we have supposed that the fluid obeys the Ostwald-De-Waele model, named also power-law model and given by:

$$\tau_{ij} = \mu_a D_{ij} = K (D_{kl} D_{kl} / 2)^{(n-1)/2} D_{ij} \tag{5}$$

Where $D_{ij} = (\partial u_i / \partial x_j + \partial u_j / \partial x_i)$, the rate of strain tensor, K is the fluid consistency, n is the power-law index and μ_a is the apparent viscosity given by:

$$\mu_a = K (D_{kl} D_{kl} / 2)^{(n-1)/2} \quad (6)$$

For $n < 1$, apparent viscosity decreases with increasing shear-rate and thus fluid is referred to as shear-thinning. For $n > 1$, apparent viscosity increases with shear-rate and fluid becomes shear-thickening. Newtonian case is for $n = 1$.

The fluid' rheological nature, directly affects the flow shape, and thus, temperature field and heat transfer rate. So, a reformulation of the dimensionless numbers encountered in such problem is needed, to well understand the effect of the n index. Many concepts can be found in literature (cf Khezzar *et al.*, 2012; Turan *et al.*, 2011b). In this study, we have supposed a modified Rayleigh and Prandtl numbers refereed to the n index. Where:

$$Ra_n = \frac{\rho^2 c_p g \beta \Delta T L^3}{\mu_n} \quad \text{and} \quad Pr_n = \frac{\mu_n c_p}{k} \quad (7)$$

Rayleigh number, represents the ratio of buoyancy-force thermal transport strength to thermal diffusion strength while Prandtl number, depicts the ratio of momentum diffusion to thermal diffusion (Turan *et al.*, 2011b).

μ_n is a nominal viscosity, developed from a scaling analysis, that can be defined based on a characteristic shear-rate $\dot{\gamma}_{ch}$, which can be scaled as: $\dot{\gamma}_{ch} \sim u_{ch} / L$, where u_{ch} is a characteristic velocity scaled as: $u_{ch} \sim \alpha / L$ (Ng and Hartnett, 1986; Lamsaadi *et al.*, 2006a; 2006b). Hence we obtain:

$$\mu_n = K \dot{\gamma}^{n-1} \sim K (\alpha / L^2)^{n-1} \quad (8)$$

α is the thermal diffusivity ($k / \rho c_p$).

Using equation (8) into equations (7), we obtain Rayleigh and Prandtl numbers' expressions used in the current study:

$$Ra_n = \frac{g \beta \Delta T L^{2n+1}}{\alpha^n (K / \rho)} ; \quad Pr_n = \frac{K}{\rho} \alpha^{n-2} L^{2-2n} \quad (9)$$

2.1 Boundary conditions

According to initial cavity position $\phi = 0^\circ$, vertical walls are at fixed and different temperatures while the horizontal ones are insulated. For the flow, no-slip condition is supposed at all walls. Then, problem boundary conditions are:

$$\begin{aligned}
(x=0, y) &\rightarrow u_1 = u_2 = 0.0 ; T = T_H \\
(x=L, y) &\rightarrow u_1 = u_2 = 0.0 ; T = T_C \\
(x, y=0) &\rightarrow u_1 = u_2 = 0.0 ; \partial T / \partial y = 0 \\
(x, y=L) &\rightarrow u_1 = u_2 = 0.0 ; \partial T / \partial y = 0
\end{aligned} \tag{10}$$

2.2 Heat transfer coefficient

For non-Newtonian power-law fluid natural convection, in cavity, dimensional analysis can show that heat transfer coefficient (Nu), is function of n , Ra_n and Pr_n . It is given by:

$$Nu = \frac{L}{(T_{wall} - T_{ref})} \left| \frac{\partial T}{\partial x} \right|_{wall} \tag{11}$$

In the present study, reference temperature is taken T_C .

Since temperature is not uniformly distributed in the fluid close to walls, and hence thermal flux, mean Nusselt number calculation is very interesting. This later is calculated by:

$$\overline{Nu} = \frac{1}{(T_{wall} - T_{ref})} \int_0^L \left| \frac{\partial T}{\partial x} \right|_{wall} dx \tag{12}$$

3. Resolution procedure

Conservation mass, momentum and energy equations, are solved numerically using a finite volume code. A second-order central differencing scheme is used for the diffusive terms, while a second-order up-wind scheme is used for the convective terms. SIMPLE Algorithm (Patankar, 1982) is employed to treat the coupled' pressure-velocity set of equations. Convergence residual values, are chosen 10^{-7} for mass and momentum parameters, and 10^{-9} for energy one. The choices are motivated by the flow perturbations caused by n decrease, Ra_n increase and ϕ change. One can choose less or more strict residual values for other cases.

3.1 Mesh independency study

To choose the optimal mesh that ensures accuracy/short-calculation-time, we have tested several meshes at first. In Table 1, only some of the tested cases have been presented, to avoid overloading the article. We note that for all the tested meshes, an amplification factor equal to 1.02 starting from walls is taken. So, the mesh is fine close to the four walls, without being coarse in the middle. The idea of this choice is the fact that the strong gradients of velocity and temperature are close

to the walls, particularly for strong Ra_n , small n in addition to cavity inclination. But, flow continuity inside the cavity, leads to considerable disturbances far from walls, where a good mesh sizing is required too.

The presented cases, are done with $Ra_n=10^{+6}$ and three angles ϕ (0° , $+30^\circ$ and -30°). Two n values are taken; $n=0.6$ for $Pr_n=1000$ and $n=1.8$ for $Pr_n=100$. The two n values, are the smallest and biggest limits of its range of variation, whereas the value of Ra_n is the largest one assumed in this study, which ensures to remain in the laminar regime (see Turan *et al.*, 2011b, 1052-1054). Pr_n values are just for variety.

For the first case, we have presented the values of \overline{Nu} and V_{maxc} (maximum dimensionless velocity in the whole cavity), for four meshes, $M_1(N_x \times N_y=101 \times 101)$, $M_2(121 \times 121)$, $M_3(141 \times 141)$ and finally $M_4(161 \times 161)$, for the three considered ϕ values. From the table, one can clearly see the closeness between M_3 and M_4 results, while clear differences are registered compared to M_2 and M_1 . We note that M_3 has nearly 24% fewer nodes compared to M_4 , therefore, a good time saving. For the second case, one can see that all meshes lead to a close results (U_2 , is the dimensionless vertical velocity). This is not surprising, since this big n value leads to high motion resistance by viscosity increase, which goes against the effect of Ra_n . This could be clearly understood along this work. We note that our results for M_3 , are compared to those in the work of Turan *et al.* (2011b), for a very fine regular mesh (200×200 elements), where very good agreement is recorded.

Table 1. Mesh independency study' tested cases. $Ra_n=10^{+6}$.
a: (Turan *et al.*, 2011b,1052 (Mesh: 200×200))

		M1 (101×101)	M2 (121×121)	M3 (141×141)	M4 (161×161)	
$n=0.6 ; Pr_n=1000$	$\phi=0^\circ$	\overline{Nu}	34.9709	36.7751	37.9431	38.1282
		V_{max-c}	2550.6878	2602.1846	2647.2583	2660.3632
	$\phi=+30^\circ$	\overline{Nu}	36.3935	37.5512	38.2151	38.2821
		V_{max-c}	3392.9090	3397.0928	3400.5262	3429.3485
	$\phi=-30^\circ$	\overline{Nu}	21.5179	22.2436	22.7725	23.2801
		V_{max-c}	1702.8200	1526.9972	1447.9440	1447.8209
$n=1.8 ; Pr_n=100$	$\phi=0^\circ$	\overline{Nu}	25.1744	2.5247	2.5137	2.4994
		$U_{2max-y=L/2}$	24.4347	27.5201	27.5141	27.5063
	$\phi=+30^\circ$	\overline{Nu}	2.6507	2.6516	2.6355	2.6170
		$U_{2max-y=L/2}$	32.5913	32.6455	32.6472	32.6667
	$\phi=-30^\circ$	\overline{Nu}	2.0297	2.0447	2.0422	2.0358
		$U_{2max-y=L/2}$	18.5335	18.5587	18.4863	18.4973

3.2 Validations

After choosing the optimal mesh, many validations were made, to be confident with the new results provided here. As it is well known, different parameters are involved in this study. This is the cause of the large number of publications in this type of problems (natural convection in square cavities for a power-law fluid). Therefore, two validations of large significations have been presented here (Fig.2), to avoid producing several ones, in order to save work size. The first validation with that produced by Turan *et al.* (2011b,1059), is for the mean Nusselt number (\overline{Nu}) calculated for seven (07) values of index n , starting from 0.6 until 1.8 with a 0.2 step, and ten (10) well distributed values of Ra_n , from 10^{+3} to 10^{+6} . Prandtl number (Pr_n) considered equals 10^{+3} and $\phi=0^\circ$. The two results comparison, exhibits a very good closeness between the obtained results and those refereed to. We note that the figure vertical velocity ($U_2=u_2L/\alpha$) at $y=L/2$ for the same n values taken for the first production is done with eighty (80) mean Nusselt number' calculations, which points-out our code' rightness. The second validation, is made for the dimensionless validation, for $Ra_n=10^{+6}$, $Pr_n=100$ and $\phi=0^\circ$ with the work of Turan *et al.* (2011b,1056). Here as well, almost identical results were obtained. For more validations, the interested reader can make use of the work of Horimek *et al.* (2016).

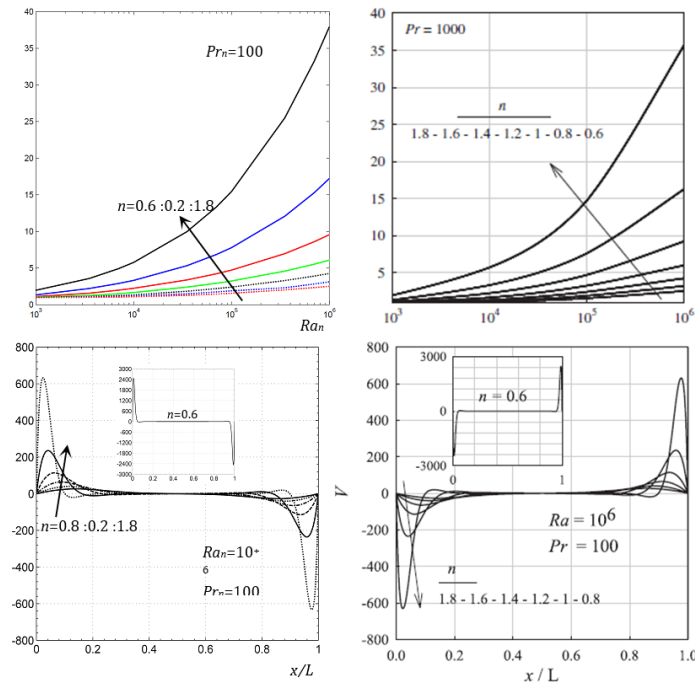


Figure 2. Comparison of our results (left) and those of Turan *et al.* (2011b). Top: \overline{Nu} ; Bottom: U_2 at $y=L/2$

4. Results and discussion

For a better exploitation of the obtained results, and in order to illustrate the effects of the many intervening parameters, this part of the work is divided into five (05) parts, where independent parameter effects' results, are presented with their physical interpretations. We note that we have chosen to present results for flow (streamlines) and thermal (isotherms) fields and keep that of mean Nusselt number (\overline{Nu}) at last, to put them together in the same figure, which makes their understanding clearer, and shows their influence magnitudes' levels.

4.1 Effect of the Rayleigh number Ra_n

In figure (3), we have presented, the dynamic (dimensionless streamlines) and thermal (isotherms) fields for $Ra_n=10^3$, 10^4 , 10^5 and 10^6 , in the case of Newtonian fluid ($n=1.0$) and no-inclination ($\phi=0^\circ$) for $Pr_n=10^3$. As said above, Rayleigh number represents the ratio of buoyancy-force thermal transport strength to thermal diffusion strength. Thus, low Ra_n value means a small magnitude of the buoyancy term compared to the diffusion term. This, leads to a tendency towards the pure-conductive heating mode as faster as Ra_n is small. For the present phenomenon, temperature gradient, in addition to density temperature-dependency, generate an ascendant motion close to the hot wall, and a decedent one close to the cold wall. Continuity inside the cavity transmits the motion to the whole zones. So, the intensity of the generated motion increases, leading to a clearer perturbation with increasing Ra_n . For this, one can see circular uniform streamlines for low Ra_n and perturbed ones when it is big. The two circulating zones seen for $Ra_n=10^5$ and 10^6 , are the direct effect of high intensities of the two flows (ascending and descending), when circulation shorts the path to be followed by the fluid particles in either flows. Consequently, the two circulating zones move towards the hot and cold walls with the enlargement of the core zone, under intensity increase (Ra_n increase). Problem coupled nature involves the thermal field perturbation, when the dynamic field is, and inversely. For this, one can see a low disturbed thermal field (isotherms) for $Ra_n=10^3$ and 10^4 and a clearly disturbed for $Ra_n=10^5$ and 10^6 .

Concerning heat transfer coefficient, it can easily be understood that it is even better as Ra_n is more important, by increasing agitation (intensified convection), and hence better mixing, which reduces fluid temperature close to hot wall, that allows more heat flux introduction. The opposite happens close the cold wall (compare the red and blue areas thicknesses on left and right sides). Mean Nusselt number (\overline{Nu}) curves are left to the end to save space (see Fig.7, for $n=1.0$ at $\phi=0^\circ$).

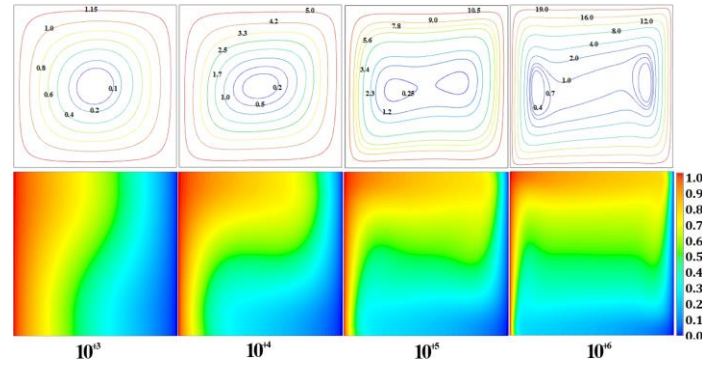


Figure 3. Rayleigh number (Ra_n) effect on dynamic field (Top) and thermal field (Bottom). $n=1.0$; $\phi=0^\circ$; $Pr_n=10^{+3}$

4.2 Effect of the rheological index n

Index n variation effects on the dynamic (streamlines) and thermal (isotherms) fields are presented in figure (4), for $Ra_n=10^{+5}$, $\phi=0^\circ$ and $Pr_n=10^{+3}$. From streamlines sub-figures (Fig.4-Top), one can see that, fluid shear-thinning (n decreases) leads to an increasing perturbation in the dynamic field. As described previously, flow intensity increase, leads to the formation of two circulating zones, becoming far each-other as Ra_n increases, while there is only one circulating zone for low intensities. Here again, but with a single Ra_n value, one can see two circulating zones for n (1.0, and only one for $n>1.0$). So, the n decrease has a similar effect to that of Ra_n increase. This can be explained from the rheological law of the fluid ($\mu_a = K \dot{\gamma}^{n-1}$). When n decreases, fluid viscosity decreases and leads to frictions reduction close to walls and between fluid' layers. Flow motion becomes easier and thereby its intensity increases. The opposite happens when n increases, since viscosity increases too. We note that n increase (decrease) effect is more important close to walls (see streamlines magnitudes in figure 4 and figure 7 in Horimek *et al.* (2016)), where velocity parietal gradient ($\dot{\gamma} = \partial u_i / \partial x_j$) is higher. From the above explanations, a faster tendency toward turbulent regime is registered when n decreases, and the opposite when it increases. So, precautions should be taken into account when dealing with such kind of fluids to stay in the laminar regime supposition. As said before; the problem is of a coupled nature. Hence, any disturbance in the dynamic field is reflected on the thermal field. This later becomes more disturbed when n is small and less disturbed in the other case (Fig.4-Bottom). Finally it becomes evident that heat transfer rate enhances with fluid shear-thinning ($n \downarrow$).

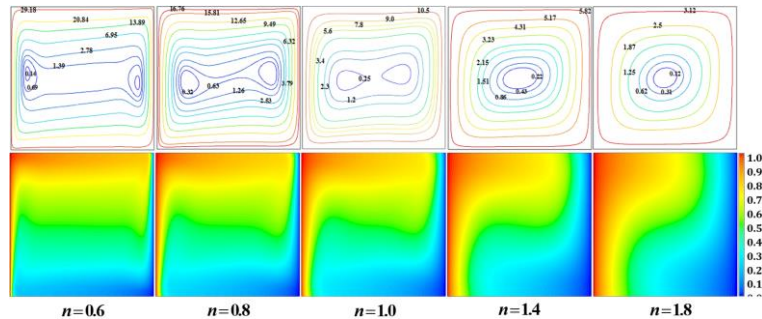


Figure 4. Effect of the rheological index (n) on dynamic field (Top) and thermal field (Bottom). $\phi=0^\circ$; $Ra_n=10^{+5}$; $Pr_n=10^{+3}$

4.3 Effect of the inclination angle ϕ

In figure (5), we have presented the effect of inclination on the dynamic and thermal fields for $Ra_n=10^{+5}$, $n=1.0$ and $Pr_n=10^{+3}$. We note that, inclination angles are presented from 0° to 85° in the counter-clockwise direction counted as positive inclination (**a**), and the same in clockwise direction counted as negative inclination (**b**). Results are presented for each 15° stepp. We note also that, $\phi=+90^\circ$ and $\phi=-90^\circ$ cases, are not presented to keep sub-figures' sizes acceptable and because they are very close to $\phi=+85^\circ$ and $\phi=-85^\circ$ cases respectively. For the first inclination case, hot wall becomes progressively down and the cold one up. So, ascending hot flow deviation caused by upper horizontal adiabatic wall (when $\phi=0^\circ$) declines progressively. The same happens for descending cold flow. As a result, the heating area length increases on left side and the same for cooling area on the right, they thicknesses decreases (see isotherms' sub-figures). Thus, density decrease in the hot side (and decrease on the cold side) leads to flow intensification. This is the reason for higher recorded magnitudes when ϕ increases. It is worth to notice, that for this case, flow intensification doesn't produce two circulating zones and the initial ones observed at $\phi=0^\circ$ have gradually disappeared. This could be explained by the fact that hot ascending and cold descending currents are of smoother motions, which lead to soft flow perturbation (see green and light blue zones enlargements with increasing ϕ). We note that, these observations tend to stabilize after a certain angle, with the recording of a red zone enlargement on the left side (blue on the right side) close to $\phi=+90^\circ$, that leads to heat exchange decrease, by temperature difference decay between hot wall and the adjacent fluid (likewise for the cold side). Consequently, heat transfer will increase to a highest value (optimal heat transfer rate) and then decreases.

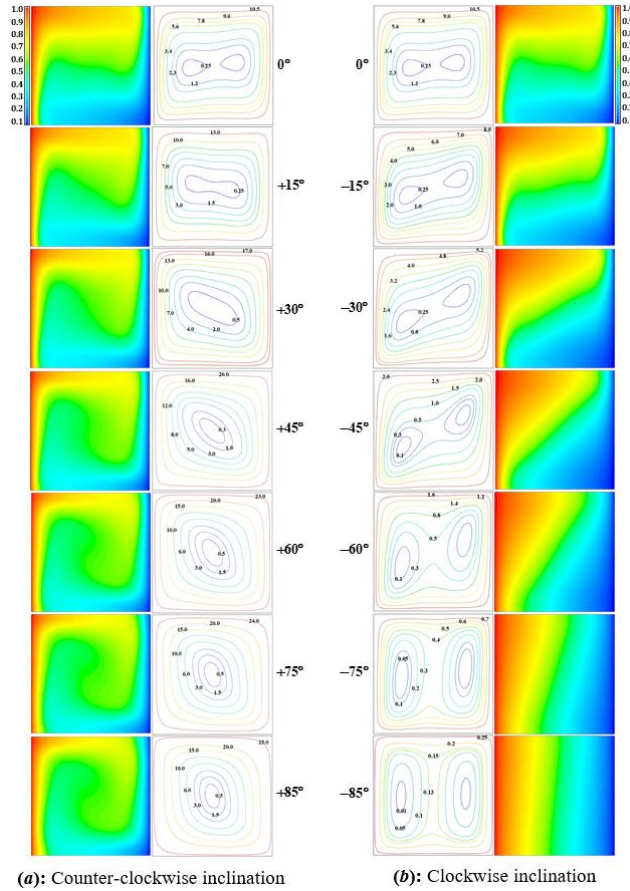


Figure 5. Effect of the inclination angle ϕ on dynamic field (Top) and thermal field (Bottom). $n=1.0$; $Ra_n=10^{+5}$; $Pr_n=10^{+3}$

For clockwise inclination direction, the opposite happens. The hot and cold walls initially vertical (left and right), have tendency to be horizontal. As well known, natural convection acts vertically (opposite to gravity vector), and the hot fluid rises up. So, when inclination angle increases, buoyancy- force decreases by a $\sin(\phi)$ factor, without restitution due to path length reduction, since hot fluid starts descending as faster as ϕ is greater (it reaches the perpendicular adiabatic wall before increasing in strength compared to the initial situation at $\phi=0^\circ$). For important values of ϕ angle, buoyancy force becomes very weak, as hot fluid almost becomes horizontal. On flow streamlines subfigures (Fig.5-b-), one can see an ongoing and significant decrease of flow intensity with respect of ϕ . The two circulating zones seen initially ($\phi=0^\circ$), tend to be independent one from the other. In other words, circulating zone caused by hot fluid motion is free from that caused by

cold fluid motion. This situation, in addition to high intensity decay, tend the heating mode toward the pure-conductive case. Obviously, from what we have just explained, heat transfer rate will monotonically decrease for this inclination kind.

4.4 Combined effects of n and ϕ

In figure (6), the combined effects of the index n and the inclination angle ϕ are presented for $Ra_n=10^{+5}$ and $Pr_n=10^{+3}$. As expected from the precedent parts, the flow perturbation and hence the thermal one increases with a counterclockwise inclination as n decreases. The opposite happens when inclination is done in clockwise direction and/or n increases. For the presented results, one can see the huge difference for flow intensities between the case $n=0.6$, $\phi=60^\circ$ and the case $n=0.6$, $\phi=-60^\circ$. Where the maximum intensity (close to the maximum), in the first case is almost 25 times that for the second case. This value is nearly 14.4 for $n=1.0$ and nearly 3.2 for $n=1.8$. This, indicates that inclination effect is more pronounced for a pseudoplastic ($n<1.0$) fluid compared to a Newtonian one. The dilatant fluid ($n>1.0$) exhibits the lowest effect. In addition, the high flow intensities for positive ϕ values (counterclockwise inclination) and pseudoplastic fluid accelerate the transition to turbulent flow. We note here that results are for $Ra_n=10^{+5}$ and the registered intensities will be greater if this later increase. In the other side, a faster tendency toward the pure conductive heating mode (0 flow), happens if the fluid is more dilatant especially when ϕ increases in the clockwise direction. For the above explanation, it becomes clear that thermal perturbation (better mixing) increases with the decreases of n and/or counterclockwise inclination, and decreases with n increase and/or clockwise inclination.

In figure (7), we have presented the evolution curves of mean Nusselt number (\overline{Nu}) depending on inclination angle ϕ . A 5° step is taken from $\phi=-90^\circ$ to $\phi=+90^\circ$. Four (04) values of Ra_n are considered, for the already seven (07) supposed n values. As expected, heat exchange improves when n decreases, due to flow agitation increase by viscosity decrease (part 4.2), in addition to better thermal mixture, which reduces fluid temperature close to hot wall, and hence more important heat flux is introduced (a more important is extracted from the cold wall for the same reason). Ra_n increase, leads to the same observations, since it favors the flow agitation and therefore better thermal mixing (part 4.1). It is obvious that the combination of the two effects, offers a greater heat exchange, compared to their effects separated. An important result can be drawn from Fig.7' sub-figures, that can be summarized in the existence of an optimal angle, which gives the greatest value of \overline{Nu} between 0° and $+90^\circ$ (counter-clockwise inclination). This result confirms what we have discussed in the bibliographic research.

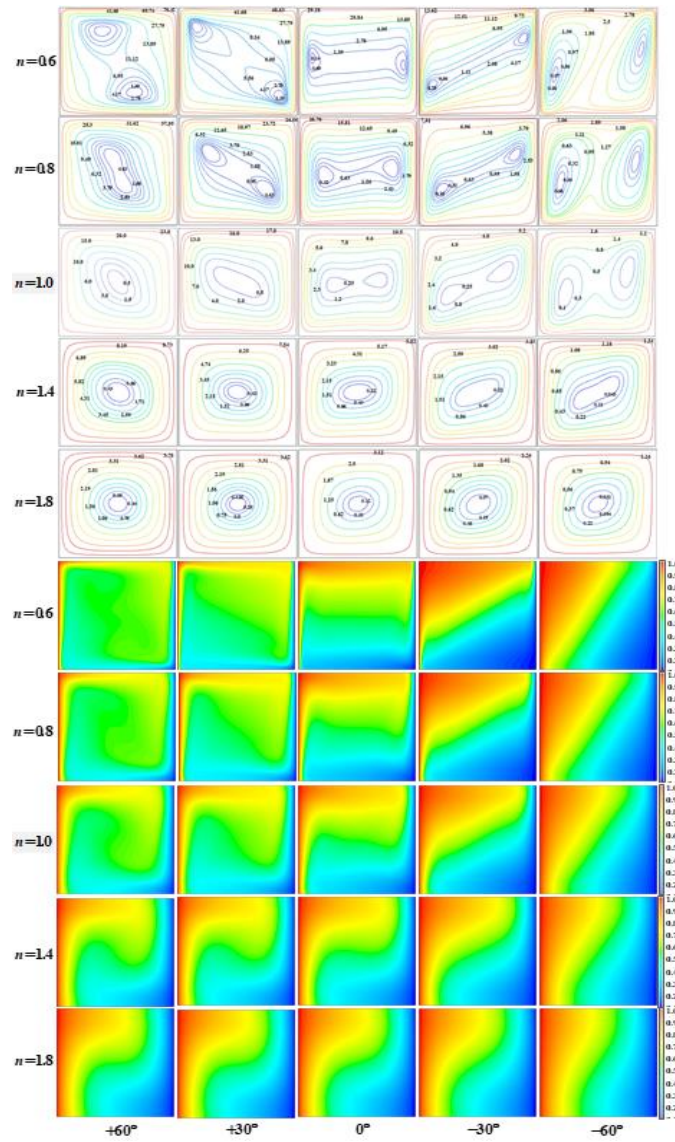


Figure 6. Combined effects of n and ϕ on dynamic field (Top) and thermal field (Bottom). $Ra_n=10+5$; $Pr_n=10+3$

Before discussing this result in detail, we report other results deemed as important. One of them is that all Nusselt curves tend towards the value 1.0 for $\phi=-90^\circ$, corresponding to hot top wall and cold bottom one, and this, whatever Ra_n and n values are. This indicates that this cavity position eliminates both Ra_n and n

effects. In other words, pure-conductive mode is produced. This result can be explained by the fact that natural convection acts vertically, and when hot wall is top, hot fluid cannot move upward in addition to wall impermeability. Same explanation at the bottom. From $\phi=0^\circ$ to $\phi=-90^\circ$, Nusselt decreases for all the considered cases until the value 1.0. As explained in part (4.3) of this work, this is the direct cause of flow intensity reduction according to ϕ .

The second noticed result is for $\phi=+90^\circ$, corresponding to cold top wall and hot bottom one, where one can see that \overline{Nu} values are nearly one (1.0), for $Ra_n=10^{+3}$ for all the considered n values. The effect of n is extinguished for this case. The physical explanation of this result is that since natural convection acts vertically, and hot wall is bottom, the fluid that undergoes a decrease in density tends to rise upward, but its intensity remains very weak (low Ra_n), it cannot yet disturb the upper-fluid' layers acting in opposite direction. So, a critical Rayleigh value must be reached to start motion. For higher Ra_n values, \overline{Nu} increase is observed. The rising hot fluid succeeds overcoming upper-fluid' layers opposing effect on its path. It is obvious that the resulting intensities will be greater when n decreases. Critical Ra_n decreases as n decreases and vice versa. As an example for $Ra_n=10^{+4}$, the cases with $n=1.6$ and $n=1.8$ are still in pure-conductive mode, whereas for the other values of n , the mode is convective, more clearly when n is smaller.

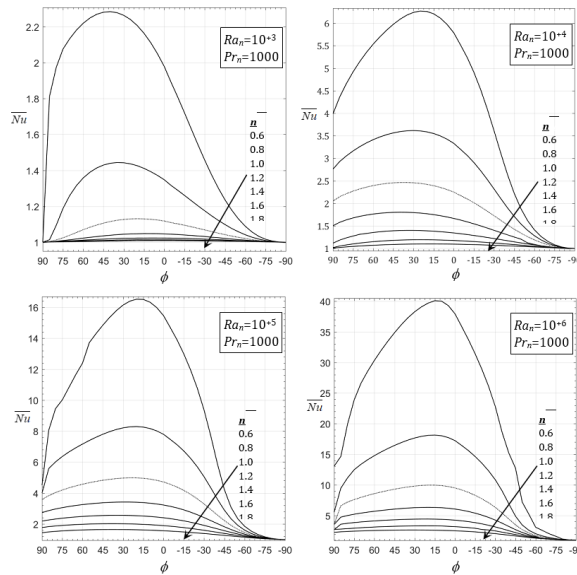


Figure 7. Mean Nusselt number (\overline{Nu}) evolution according to inclination angle (ϕ) for different n and Ra_n . $Pr_n=10^{+3}$

Let's return to the observation mentioned above. As well known, Nusselt increase is caused by a stronger agitation with flow intensity increase, especially

near the walls (where \overline{Nu}). In addition, better thermal mixture reduces temperature near the hot wall (the opposite close to the cold wall), and hence more thermal flux is absorbed resulting of temperatures difference increase between the wall and the adjacent fluid layers. Keeping the same parameters (n , Ra_n and Pr_n) and tilting the cavity left (counter-clockwise), fluid will be more agitated as discussed in Part (4.3). Nusselt starts to increase until a certain angle, then decreases until its lowest values at $\phi=+90^\circ$. This can be explained by the fact that when cavity is inclined to the left, hot ascending fluid path length increases. Therefore, the solicited zone where fluid density is affected by hot temperature becomes longer, which leads to further flow intensification. In addition, adiabatic top horizontal wall, progressively turns toward vertical situation, hot ascending fluid' path becomes smoother and circulating zone (initially two) becomes only a big one, but with increasing intensity (see magnitudes). Core zone becomes more heated (green and light-blue colors) compared to the initial situation ($\phi=0^\circ$). A better mixture results and as consequence, heat transfer rate increases progressively. After a certain tilting angle, stabilization is reached with an increase of fluid temperature close to hot wall, which reduces the heat transfer rate. The given explanation still valid in general, but Nusselt curves analysis from Fig.7 for all the treated cases, shows that optimal value is reached at higher inclination angles when Ra_n is small ($\phi \approx +45^\circ$ for $Ra_n=10^{+3}$ and $\approx +30^\circ$ for $Ra_n=10^{+4}$) compared to the other cases, where it becomes increasingly close to $\phi=0^\circ$ (precisely $\approx +15^\circ$) with Ra_n increase, especially when n is smaller. This is due to combined effects of ϕ angle, Ra_n number and n that increase flow agitation faster.

4.5 Effect of Prandtl number (Pr_n)

In this last part, we have presented the effect of Prandtl number (Pr_n) on mean Nusselt number (\overline{Nu}), for different values of the inclination angle ϕ (7 values are taken), but only for $Ra_n=10^{+5}$. We note that the choice of Ra_n value is motivated by the fact that natural convection is strong enough to alter the flow, hence a well analysis. Furthermore, all other parameters are amply discussed above. In addition, and following the work of Turan *et al.* (2011b,1059-1060), Prandtl number does not have a sensitive effect on Nusselt number for values $\gg 1$ (very low effect on both dynamic and thermal fields). The explanation of this is that for $Pr_n \gg 1$, thermal boundary layer thickness is very small compared to the dynamic one. So, a Pr_n increase will not change much the balance between viscous and buoyancy forces inside the thermal boundary layer. On the other hand, for relatively low Pr_n values ($< 10^{+2}$), the two boundary layers (dynamic and thermal) are close in thicknesses; any Pr_n modification will be therefore reflected on the Nusselt number. In addition, for a very small Pr_n ($O(1)$), a risk of transition to turbulent regime is presented, especially for high Ra_n . It is noted that the rheological index (n) decrease, reduces viscous forces and thus favors the disruptive effect. Osman *et al.* have reported numerical instabilities for the case $Pr_n=10$, $n=0.6$ at $Ra_n=10^{+6}$ (cf Turan *et al.*,2011b,1059). From the above details, Pr_n was between 10 and 10^{+4} , which is largely sufficient to illustrate its effect in presence of an inclination.

From figure (8), one can see an increase of \overline{Nu} when Pr_n increases, but only for pseudoplastic fluid ($n < 1.0$). This effect is clearer when n is smaller. The physical explanation of this observation is the fact that when n decreases, thermal boundary layer thickness decreases too (cf Horimek *et al.* (2015)). Pr_n decrease has an opposite effect. So, the two opposite effects combination leads to a clearer Nusselt modification. For n values ≥ 1.0 , no Pr_n is recorded. Simply because of the n negligible effect on the thermal boundary layer. A careful analysis of the figure, allows us to see that Pr_n effect when n is small is more important close the optimal angle compared to the other angles. This is the direct effect of parietal velocity gradient ($\dot{\gamma}$) increase close the walls, when flow intensity increases in a thinner solicited zone (see our explanations in part 4.3).

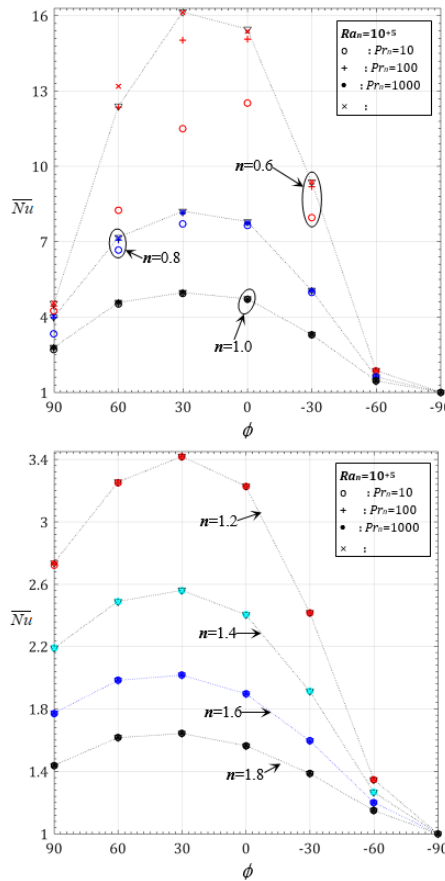


Figure 8. Prandtl number (Pr_n) effect on mean Nusselt number (\overline{Nu}) for different n and ϕ values. $Ra_n = 10^{+5}$

At this work end, we can say that to ensure a maximum heat transfer rate, we have to know at first, the fluid physical properties (n , K , ρ , ...), assuming $(T_H - T_C)$ known. Therefore, Ra_n and Pr_n values are determined. If Pr_n exceeds 10^{+2} , we will act directly on cavity inclination in counter-clockwise direction. But, we have to check the Ra_n value. If it is $\leq 10^{+4}$, inclination must be between 15° and 55° for all n values. If it exceeds 10^{+5} , it must be between 5° and 20° . Between 10^{+4} and 10^{+5} , the range of 10° to 35° seems good. For a $Pr_n < 10^{+2}$, we must think to increase Ra_n , by increasing $(T_H - T_C)$ for the same ranges of inclination angle above-mentioned, if $n < 1.0$, especially as n is small. The fact of proposing ranges implies that one has bounded the optimal \overline{Nu} , a slight loss in the rate of heat exchange does not really annoy.

5. Conclusions

Laminar natural convection problem, for an inclined differentially heated square cavity, filled with a power-law fluid, has been numerically studied. The study allowed concluding that:

Flow and thermal fields are more disturbed when Ra_n increases, by buoyancy-force effect;

Fluid shear-thinning ($n \downarrow$) leads to similar observations, by friction reduction close to walls and between fluid layers;

Counter-clockwise inclination, increases flow and thermal fields' perturbations by hot and cold fluid paths increase, in addition to motions smoothing compared to case $\phi = 0^\circ$, followed by little decrease in perturbations close to $\phi = +90^\circ$. A monotonically decrease in perturbations is recorded for the clockwise inclination;

Mean heat transfer rate increases when Ra_n increases and/or n decreases for both inclinations. For counter-clockwise inclination, Nusselt increases until an optimal value and then decreases, while it decreases monotonically for the clockwise inclination until the pure-conductive mode value;

Pr_n number has only a clear effect when it is small ($< 10^{+2}$), but only for a pseudoplastic fluid ($n < 1.0$), by opposing effects between them (Pr_n and n). This is clearer close to the optimal inclination angle;

Lastly proposed ranges of the inclination angle may help to ensure an optimal heat transfer rate, depending on the problem' parameters' value.

References

- Hamady F. J., lloyd J. R., Yang H. Q., Yang K. T. (1989). Study of local natural convection heat transfer in an inclined enclosure. *International Journal of Heat and Mass Transfer*, Vol. 32, No. 9. pp. 1697-1708. [http://dx.doi.org/1016/0017-9310\(89\)90052-5](http://dx.doi.org/1016/0017-9310(89)90052-5)
- Horimek A., Ait-Messaoudene N., Aich W., Aichouni M., Kolsi L., Ghernaout J. (2015). Laminar forced convection of a pseudoplastic thermodependent fluid in an annular

- horizontal duct. *Arab Gulf Journal of Scientific Research*, Vol. 33, no. 4, pp. 125-137. http://dx.doi.org/1007/978-3-319-70950-5_7
- Horimek A., Noureddine B., Benkhchiba A., Ait-Messaoudene N. (2016). Natural convection for an Oswald-De-Waele fluid inside a differentially heated square cavity. *International Conference on Mechanics and Energy (ICME'2016)*, Hammamet, Tunisia, reference. ICME2016-85.
- Huelsz G., Rechtman R. (2013). Heat transfer due to natural convection in an inclined square cavity using the lattice Boltzmann equation method. *International Journal of Thermal Science*, Vol. 65, pp. 111-119. <http://dx.doi.org/1016/j.ijthermalsci.2012.09.009>
- Kaddiri M., Naïmi M., Raji A., Hasnaoui M. (2012). Rayleigh-Benard convection of non-Newtonian power-law fluids temperature-dependent viscosity. *ISRN Thermodynamics*, Vol. 2012, No. 614712-10. <http://dx.doi.org/5402/2012/614712>
- Khezzar L., Siginer D., Vinogradov I. (2011). Natural convection in inclined two dimensional rectangular cavities. *Heat and Mass Transfer*, Vol. 48, No. 2, pp. 227-239. <http://dx.doi.org/1007/s00231-011-0876-7>
- Khezzar L., Siginer D., Vinogradov I. (2012). Natural convection of power law fluids in inclined cavities. *International Journal of Thermal Science*, Vol. 53, pp. 8-17. <http://dx.doi.org/1016/j.ijthermalsci.2011.10.020>
- Koca A., Oztop H.F., Varol Y. (2007). The effects of Prandtl number on natural convection in triangular enclosures with localized heating from below. *International Communication in Heat Mass Transfer*, Vol. 34, pp. 511-519. <http://dx.doi.org/1016/j.icheatmasstransfer.2007.01.006>
- Lamsaadi M., Naimi M., Hasnaoui M. (2006). Natural convection heat transfer in shallow horizontal rectangular enclosures uniformly heated from the side and filled with non-Newtonian power law fluids. *Energy Conversion and Management*, Vol. 47, No. 15-16, pp. 2535-2551. <http://dx.doi.org/1016/j.enconman.2005.10.028>
- Lamsaadi M., Naimi M., Hasnaoui M., Mamou M. (2006). Natural convection in a vertical rectangular cavity filled with a non-Newtonian power law fluid and subjected to a horizontal temperature gradient. *Numerical Heat Transfer, Part A*, Vol. 49, No. 10, pp. 969-990. <http://dx.doi.org/1080/10407780500324988>
- Ng M. L., Hartnett J. P. P. (1986). Natural convection in power law fluids. *International Communication in Heat and Mass Transfer*, 13, no. 1, pp. 115-120. [http://dx.doi.org/1016/0735-1933\(86\)90078-3](http://dx.doi.org/1016/0735-1933(86)90078-3)
- Ohta M., Ohta M., Akiyoshi M., Obata E. (2002). A numerical study on natural convective heat transfer of pseudoplastic fluids in a square cavity. *Numerical Heat Transfer, Part A*, Vol. 41, No. 4, pp. 357- 372. <http://dx.doi.org/1080/104077802317261218>
- Ostrach S. (1972). *Natural convection in enclosures*. in: J.P.P. Hartnett, T.F. Irvine (Eds.), *Advances in Heat Transfer*, 8. Academic Press, London.
- Ozoe H., Churchill S.W. (1972). Hydrodynamic stability and natural convection in Ostwald-De Waele and Ellis fluids: the development of a numerical solution. *AIChE Journal*, Vol. 18, No. 6, pp. 1196-1207. <http://dx.doi.org/1002/aic.690180617>
- Patankar S. V. (1982), *Numerical Heat Transfer and Fluid Flow*, Hemisphere, Washington, DC.

- Raisi A. (2016). Natural convection of non-Newtonian fluids in a square cavity with a localized heat source. *Journal of Mechanical Engineering*, Vol.62, No. 10, pp. 553-564.
- Rasoul J., Prinos P. P. (1997). Natural convection in an inclined enclosure. *International Journal of Numerical Method for Heat and Fluid Flow*, Vol. 7, No. 5, pp. 438-478. <http://dx.doi.org/1108/09615539710187783>
- Turan O., Poole R. J., Chakraborty N. (2011). Influences of boundary conditions on laminar natural convection in rectangular enclosures with differentially heated side walls. *International Journal of Heat and Fluid Flow*, Vol. 33, No. 1, pp. 131-146. <http://dx.doi.org/1080/01457632.2014.852870>
- Turan O., Sachdeva A., Chakraborty N., Poole R. J. (2011). Laminar natural convection of power-law fluids in a square enclosure with differentially heated side walls subjected to constant wall temperatures. *Journal of Non-Newtonian Fluid Mechanics*, Vol. 166, No 17-18, pp. 1049-1063. <http://dx.doi.org/1016/j.jnnfm.2011.06.003>
- Turan O., Sachdeva A., Poole R. J., Chakraborty N. (2012). Laminar natural convection of power-law fluids in a square enclosure with differentially heated side walls subjected to constant wall heat flux. *Journal of Heat Transfer ASME*, Vol. 134, No. 12, pp. 122504-122515. <http://dx.doi.org/1016/j.jnnfm.2011.06.003>
- Turan O., Sachdeva A., Poole R. J., Chakraborty N. (2013). Aspect ratio and boundary conditions effects on laminar natural convection of power-law fluids in a rectangular enclosure with differentially heated side walls. *International Journal of Heat and Mass Transfer*, Vol. 60, pp. 722-738. <http://dx.doi.org/1016/j.ijheatmasstransfer.2013.01.017>
- Vinogradov I., Khezzar L., Signiner D. (2011). Heat transfer of non-Newtonian dilatant power law fluids in square and rectangular cavities. *Journal of Applied fluid Mechanics*, Vol. 4, No. 3, pp. 37-42.
- Yener Y., Kakac S., Pramuanjaroenkij A. (2013). *Convective Heat Transfer*, Third Edition. Boca Raton: CRC Press.
- Yigit S., Graham T., Poole R. J., Chakraborty N. (2016). Numerical investigation of steady-state laminar natural convection of power-law fluids in square cross-sectioned cylindrical annular cavity with differentially-heated vertical walls. *International Journal of Numerical Method for heat and fluid flow*, Vol. 26, No. 1, pp. 85-107.
- Yigit S., Poole R. J., Chakraborty N. (2013). Laminar natural convection of Bingham fluids in inclined differentially heated square enclosures subjected to uniform wall temperatures. *Journal of Heat Transfer*, Vol. 137, No. 5, p. 052504-12. <http://dx.doi.org/1080/01457632.2016.1239937>